INTERNATIONAL JOURNAL OF MULTIDISCIPLINARY: APPLIED BUSINESS AND EDUCATION RESEARCH
2025, Vol. 6, No. 6, 3018 – 3044
http://dx.doi.org/10.11594/ijmaber.06.06.30

Research Article

Valorization of Cassava Peel and Shrimp Shell Waste for Bioplastic Film Development: Extraction, Characterization, and Response Modeling

André E. Picar, Bianca Isabel B. Molina, Joachim Florenzo C. Dejuras, Maria Julliana T. Veran, John Ray C. Estrellado*

Department of Science, Technology, Engineering, and Mathematics, The Academy,De La Salle University – Laguna, Laguna Boulevard, LTI Spine Road, Barangays Biñan and Malamig, Biñan City, Laguna, 4024, Philippines

Article history:
Submission 03 May 2025
Revised 31 May 2025
Accepted 23 June 2025

**Corresponding author:*
E-mail:
john.ray.estrellado@dlsu.edu.ph

ABSTRACT

Accumulation of waste food materials, such as cassava and shrimp peels, continues to contribute to rise in greenhouse emissions. This study aims to produce a bioplastic film made from extracted cassava peel starch (CPS) and shrimp shell chitosan (SSCHT), plasticized with sorbitol (SOR) using a constrained D-optimal mixture design. Films were assessed in terms of tensile strength, elongation at break, contact angle, opacity, and functional groups. Significant models were generated in terms of tensile strength ($p = 0.0148$), contact angle ($p = 0.1049$) and opacity ($p = 0.6529$). Cassava peel starch had a significant ($p < 0.001$) effect on tensile strength due to hydrogen bonding with chitosan, whereas elongation at break was significantly ($p = 0.0017$) affected by sorbitol due to its structural similarity to starch and larger molecular weight as compared to glycerol. Contact angle increased with the incorporation of shrimp shell chitosan ($p = 0.4647$) by minimizing hydrophilic regions for external water molecule penetration. Opacity was significantly ($p = 0.0013$) reduced by the incorporation of cassava peel starch due to the refraction of swollen starch granules. Fourier-Transform Infrared Spectroscopy (FTIR) verified the interactions in the CPS/SSCHT/SOR bioplastic film, while thermogravimetric analysis (TGA) provided insights on thermal stability of the bioplastic for industrial use. This study provides insight into the potential of food waste valorization using green extraction methods in producing environmentally friendly bioplastics for hard packaging applications.

Keywords: *bioplastic, cassava peel, shrimp shell, starch, waste valorization*

How to cite:
Picar, A. E., Molina, B. I. B., Dejuras, J. F. C., Veran, M. J. T., & Estrellado, J. R. C. (2025). Valorization of Cassava Peel and Shrimp Shell Waste for Bioplastic Film Development: Extraction, Characterization, and Response Modeling. *International Journal of Multidisciplinary: Applied Business and Education Research*. *6*(6), 3018 – 3044. doi: 10.11594/ijmaber.06.06.30

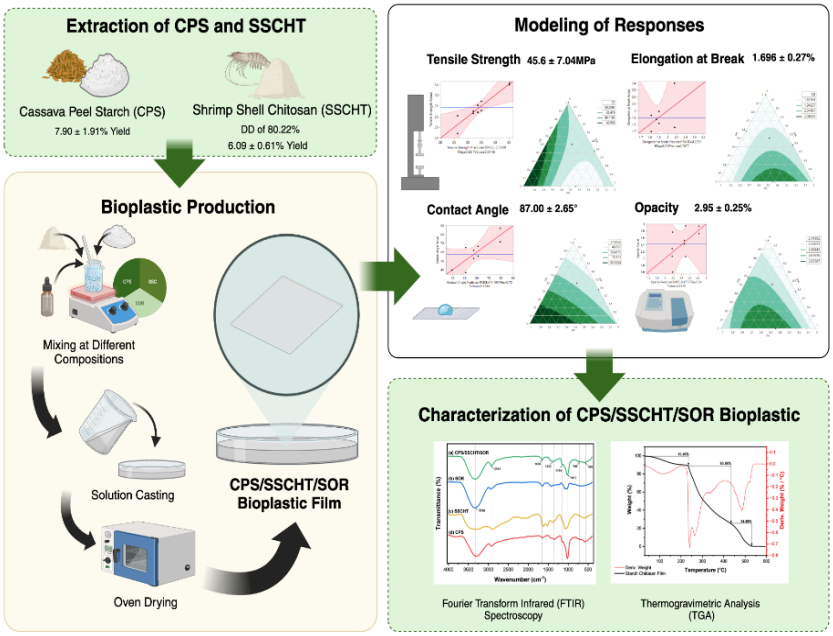

Introduction

Background of the Study

By 2050, global waste generation is expected to increase by 70% to 3.40 billion tons, which UNEP (2024) describes as the "worst scenario." The food waste crisis alone has led to approximately 931 million tons of food waste being produced every year, resulting in 8-10% of global greenhouse gas emissions (United Nations Environment Programme, 2021). Alongside food waste, annual plastic production has risen to 460 million tons a year, with about 350 million tons turning into plastic waste (Ritchie et al., 2023). As a result, plastic and food waste are two problems that go hand in hand, raising the need for innovative solutions to waste management.

Food waste valorization for bioplastic food packaging can serve to address both issues simultaneously. By treating food waste containing biopolymers, these materials hold the potential to be utilized for bioplastic production (Ramadhan & Handayani, 2020). Bioplastics developed from agri-food waste and byproducts could serve as a viable alternative to plastic packaging, due in part to its degradable or compostable nature and inexpensive materials (Jõgi & Bhat, 2020). Gerassimidou et al. (2022) conducted a study which assessed the potential of producing food loss and waste bioplastics that showcased the reality of its life cycle sustainability performance. The lack of evidence suggesting bioplastics derived from food loss and waste (FLW) are a technically feasible, economically viable, and environmentally friendly alternative may have unintended implications. This emphasizes the need for more research to make sure that FLW valorization for the production of bioplastics is a safe, sustainable, and revolutionary endeavor that might alter the plastics economy and the food system without exacerbating the issue of plastic pollution.

Food waste can be generated from all stages of the food supply chain, but the ideal materials for bioplastic production are typically derived from food processing byproducts. Cassava (Manihot esculenta) peels hold potential as a food processing byproduct due to their availability and starch content (Abel et al., 2021). According to the Department of Agriculture (2021), 1.8 million tons of cassava roots are produced from 120,000 hectares of agricultural land in the Philippines, whereas 18% of the plant itself is waste generated from processing (Oghenejoboh et al., 2021). Starch extraction from cassava peels resulted in strong intermolecular and intramolecular interactions (Fronza et al., 2022), and similar morphological properties and functional groups as that of commercial cassava starch (Thuppahige et al., 2023).

Considering this, cassava peels can be utilized as a source of starch to reduce food processing waste and improve food security.

Shrimp shells can also undergo food waste valorization. By treating shrimp shells through chemical deproteinization, demineralization, and decolorization, chitin can be extracted and converted to chitosan by deacetylation (Pakizeh et al., 2021). Shrimp waste comprises approximately 40-45% of the shrimp material weight (Wani et al., 2023), accounting for the millions of tons of waste generated by the shrimp processing industry every year (Nirmal et al., 2020). Whereas conventional methods for chitosan extraction from shrimp shells often utilize harsh chemicals that are environmentally harmful and cost-inefficient (Mohan et al., 2022), new studies have emerged promoting green and environmentally sustainable approaches to chitosan extraction (Gharbi et al., 2023).

Utilizing these two natural polymers in the production of bioplastics could allow for better optimization of essential parameters. Tan et al.'s (2022) parametric analysis revealed that starch-chitosan bioplastic films had improved tensile strength and water resistance as compared to pure-starch bioplastics. Mutmainna et al. (2019) corroborated the positive impact of chitosan on starch bioplastics, wherein mechanical strength increased as chitosan concentration increased. While these studies utilized commercial materials, this study focuses on the characterization of bioplastic food packaging films made with materials derived from food waste. Although numerous studies have emphasized the potential of food waste valorization for bioplastics (Li et al., 2022; Ramadhan & Handayani, 2020; Tsang et al., 2019), as well as the combination of cassava peel starch and chitosan for bioplastics (Pujiono & Nurhayati, 2020), there is little to no research on the food waste valorization of both cassava peel starch and shrimp shell chitosan and the impact of each material's concentration on the properties of the produced films.

Research Objectives

The objective of this research was to produce a Cassava Peel Starch (CPS)/Shrimp Shell Chitosan (SSCHT)/Sorbitol (SOR) bioplastic film utilizing a constrained D-optimal mixture design and to assess the effect of component concentration on the mechanical, optical, and wettability of the developed films. The specific objectives are as follows:

1. Extract and characterize starch from local cassava peels in terms of its functional groups and percent yield.
2. Extract and characterize chitosan from local shrimp shell waste in terms of its functional groups, degree of deacetylation, and percent yield.
3. Produce Cassava Peel Starch/Shrimp Shell Chitosan/Sorbitol (CPS/SSCHT/SOR) bioplastic films by means of a 10-point constrained D-optimal mixture design.
4. Model the tensile strength, elongation at break, contact angle, and opacity of the CPS/SSCHT/SOR bioplastic films.
5. Perform spectroscopic characterization of the CPS/SSCHT/SOR bioplastic films.

Scope and Limitations

The scope of this study was limited to the extraction and characterization of the cassava peel starch and shrimp shell chitosan, and the development and characterization of the produced CPS/SSCHT/SOR food packaging films. This study involved the comparison of valorized food waste materials to their commercial counterparts as a benchmark for the functional groups present. Considering the high cost and time required for chitosan extraction, the mixture design was constrained to account for a limited and minimal amount of chitosan. This is further explained in the methodology section of this study.

The shrimp shells and cassava peels utilized in this study were sourced from local cassava vendors and the research proponents. Only the food waste was collected as materials, and the food products (shrimp meat, peeled cassava tubers) were managed by the sources or consumed to minimize waste and avoid compromising food security.

JMP 18.1.1 was utilized as the primary software tool for the data analysis and construction of the D-optimal constrained mixture design used in this study, whereas OriginPro and GraphPad Prism were utilized for the analysis

of Fourier transform infrared (FTIR) spectra graphs.

Methods

Experimental Phases

Both quantitative and qualitative methods were utilized in the analysis of extracted materials and synthesized films. Quantitative methods include the determination of percent yield for both cassava peel starch and shrimp shell chitosan, degree of deacetylation for shrimp shell chitosan, and an analysis of variance (ANOVA) of the CPS/SSCHT/SOR films in terms of tensile strength, elongation at break, contact angle, and opacity, and the impact of each component on the film's responses. The experimental phases of the study were summarized in Figure 1.

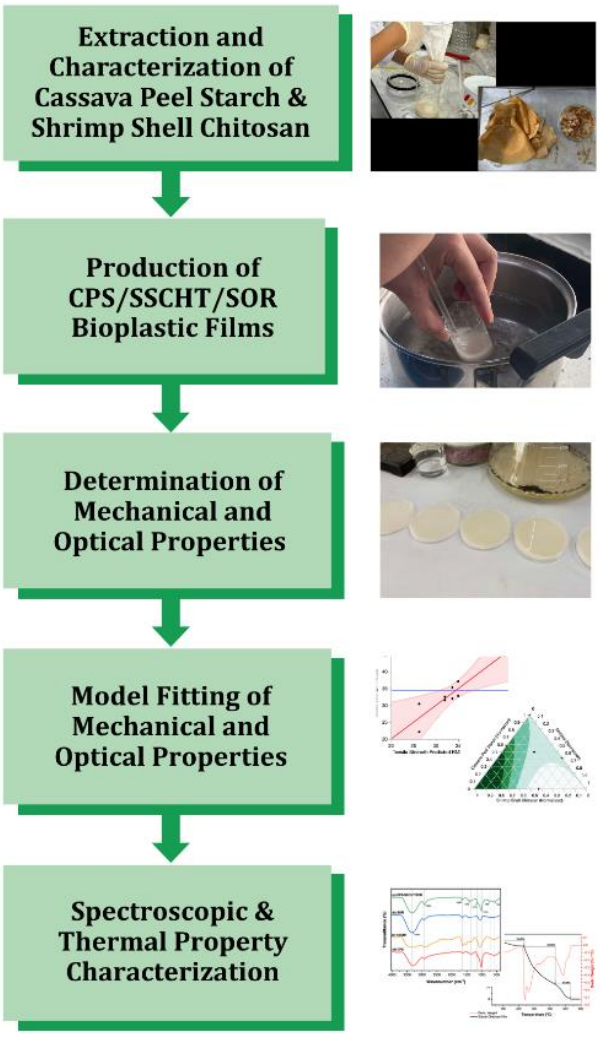

Figure 1. Production and Analysis of CPS/SSCHT/SOR Bioplastics Films

Materials

The raw materials utilized in this study were cassava peels collected from a local vendor in Sta. Rosa, Laguna, and shrimp shells were collected from the research proponents. To minimize sustainability concerns, only food processing byproducts were collected for the study. Food sources, namely the meat of the shrimp and the tuber of the cassava, are either handled by the source or consumed. The reagents used for this study include sorbitol (Fw Spavenue Inc., Makati City, Philippines), pure glycerine (PHILUSA Corporation, Pasig City, Philippines), anhydrous citric acid (Kemrad Incorporated, Quezon City, Philippines), glacial acetic acid (RCI Labscan Limited, Bangkok, Thailand), sodium chloride (RCI Labscan Limited, Bangkok, Thailand), sodium hydroxide pellets (Chem-Lab, Zedelgem, Belgium), copper(II) sulfate pentahydrate (Loba Chemie Pvt. Ltd., Mumbai, India), and potassium sodium tartrate tetrahydrate (Loba Chemie Pvt. Ltd., Mumbai, India).

Data Collection Instruments and Equipment

The equipment used for the extraction of cassava peel starch and shrimp shell chitosan were Panasonic MX-AC210S mixer grinder (Panasonic Corporation, Osaka, Japan), Scientz 18-N Freeze Dryer (Ningbo Scientz Biotechnology Co., Ltd., Zhejiang, China), and hot plate with magnetic stirrer (Torrey Pines Scientific Inc., California, United States). Determination of tensile strength and elongation at break was done using Zwick Roell Z0.5 Universal Testing Machine (Zwick Roell Group, Ulm, Germany). Scanning electron microscopy (SEM) analysis was performed using JEOL JSM 5310 Scanning Electron Microscope (JEOL Ltd., Tokyo, Japan). Opacity was determined using the Shimadzu UV-1700 Spectrophotometer (Shimadzu Corporation, Kyoto, Japan). Thermogravimetric analysis (TGA) was carried out with a TA Instruments Discovery TGA55 (TA Instruments, New Castle, DE, USA).

Experimental Design

A 10-run constrained D-optimal mixture design was applied with upper and lower bounds as a means to analyze the effects of each

component while limiting their proportions in order to maximize efficiency while minimizing redundancy. For instance, shrimp shell chitosan could not be utilized in large amounts due to the length and costs of the extraction process, or how the utilization of a plasticizer solely would not result in film formation. As such, cassava peel starch (70-82%), shrimp shell chitosan (0-5%), and sorbitol (18-25%) were limited to the given ranges based on Pelissari et al.'s (2012) design, with sorbitol in place of glycerol. Sorbitol was utilized instead of glycerol due to its lower moisture content retention (Shafqat et al., 2021) and greater mechanical strength (González-Torres et al., 2021). In order to effectively analyze the effect of each component within the experimental space, pseudo-components were computed based on Equation 1 to simplify model fitting of the constrained mixture design (National Institute of Science and Technology, 2022).

$$x_i^* = \frac{x_i - L_i}{1 - L}; L = \sum_i^n L_i < 1 \qquad \text{(Eq. 1)}$$

Wherein:
x_i^* is the Component pseudo-concentration
x_i is the Component real concentration
L_i is the Lower bound of component
L is the Sum of all components' lower bound

A 10-run constrained D-optimal mixture design was generated using JMP 18.1.1 software, with the real concentrations generated and their corresponding pseudo-components summarized in Table 1. The films were tested in terms of tensile strength, elongation at break, contact angle, and opacity. A fit model was generated for each response by Scheffe's Cubic model and interpreted in terms of analysis of variance, coefficient of determination, and regression coefficient parameter estimate to evaluate the reliability of the predictive model and the significance of each component.

Table 1. Ten-point constrained D-optimal mixture design in real concentrations and pseudo-components of CPS/SSCHT/SOR

Run	In real concentrations			In pseudo-components		
	Starch (x_1)	Chitosan (x_2)	Sorbitol (x_2)	Starch (x_{1*})	Chitosan (x_{2*})	Sorbitol(x_{3*})
BP-1	0.77	0.05	0.18	0.58	0.42	0.00
BP-2	0.70	0.05	0.25	0.00	0.42	0.58
BP-3	0.75	0	0.25	0.42	0.00	0.58
BP-4	0.82	0	0.18	1.00	0.00	0.00
BP-5	0.77	0.05	0.18	0.58	0.42	0.00
BP-6	0.76	0.025	0.215	0.50	0.21	0.29
BP-7	0.76	0.025	0.215	0.50	0.21	0.29
BP-8	0.70	0.05	0.25	0.00	0.42	0.58
BP-9	0.82	0	0.18	1.00	0.00	0.00
BP-10	0.75	0	0.25	0.42	0.00	0.58

Extraction of Cassava Peel Starch

Cassava peel starch was extracted based on Fronza et al.'s (2022) research design, wherein the cassava peel starch extraction process across its four primary stages, which consists of, washing of cassava peels, isolation of cassava peel cortex, extraction and centrifugation of the cassava peel starch extract, and lastly, drying and weighing of cassava peel starch extract. Cassava peels were processed by first isolating the cortex from the periderm. The isolated peels were then blended with distilled water in a 1:1 ratio using a Hurom H200 fruit juicer (HUROM Co., Philippines) which separated the solid pulpy residue from the liquid extract. The extract was then filtered through a cheesecloth. Peel residue undergoes repeated blending and filtration for a total of three runs. Accumulated filtrate was separated by means of centrifugation using a VS-4000i centrifuge (Vision Scientific Co., Korea) at 4,000 rpm for five min for two repetitions. The cassava peel

starch sediment was collected and freeze-dried using Scientz 18-N Freeze Dryer (Ningbo Scientz Biotechnology Co., Ltd., Zhejiang, China). Cassava peel starch was characterized in terms of its functional groups by FTIR analysis and dry basis percent yield.

Characterization of Cassava Peel Starch

The functional groups were determined based on Thuppahige et al.'s (2023) design through the use of an FTIR spectrometer positioned on the cassava peel starch sample's surface and scanned at a frequency range of 4000-450 cm^{-1}. The FTIR spectra was recorded and presented in a line graph, and compared to the spectra of commercial cassava starch (CCS) and cassava starch extract (CSE). Percent yield was determined based on Thuppahige et al.'s (2023) research design. The cassava peels were first weighed before extraction, then the finalized cassava peel starch post-extraction was weighed in comparison. The starch yield on a dry basis will be calculated with Equation 2.

$$Y_{CPS}(\%) = \frac{m_{CPS}}{m_{CP}} \times 100 \quad \text{(Eq. 2)}$$

Wherein:
Y_{CPS} is the Starch yield
m_{CPS} is the Dry weight of extracted starch
m_{CP} is the Dry weight of cassava peel

Extraction of Shrimp Shell Chitosan

Shrimp shell chitosan was extracted based on Gharbi et al.'s (2023) research design. Organs and meat were removed from the shells before boiling in 100 mL distilled water for 30 min using a hot plate (Torrey Pines Scientific, USA). Boiled shells were then dried, ground, and passed through a 60-mesh sieve. Shrimp shell powder was deproteinized and decalcified by means of a Gly/5%CA green solvent. The solution was prepared by combining 100mL 5% citric acid with 50g of glycerol, stirred, and heated to 80°C until it formed a single phase. The ground shrimp shell was treated with the Gly/5%CA solvent at 120°C for two hr, after which the solution was cooled and filtered. The resulting chitin was bleached with 3% H_2O_2 at 80°C for 90 min, then deacetylated with 60% NaOH at 100°C for four hours. Afterward, shrimp shell chitosan precipitate was filtered and neutralized in a vacuum filter and lyophilized. Shrimp shell chitosan was characterized in terms of its functional groups by FTIR analysis, degree of deacetylation, and dry basis percent yield.

Characterization of Shrimp Shell Chitosan

Determination of degree of deacetylation was modeled after William and Wid's (2019) research design. A FTIR spectrometer was utilized to scan the chitosan samples at a frequency range of 4000-450 cm^{-1}. The degree of deacetylation (DD) was calculated for at the ratio A_{1320}/A_{1420} with Equations 3 and 4. The determination of extraction yield was modeled after William and Wid's (2019) research design. The wet weight of the shrimp shell waste and the extracted chitosan were weighed and calculated with Equation 5.

$$DA(\%) = \frac{\frac{A_{1320}}{A_{1420}} - 0.3822}{0.03133} \quad \text{(Eq. 3)}$$

$$DD(\%) = 100 - DA(\%) \quad \text{(Eq. 4)}$$

$$Y_{SSCHT}\ (\%) = \frac{m_{SSCHT}\ (g)}{m_{SS}\ (g)} \times 100\% \quad \text{(Eq. 5)}$$

Wherein:
DD is the Degree of deacetylation (%)
DA is the Degree of acetylation (%)
A_{1320} is the Peak area for band 1320 cm^{-1}
A_{1420} is the Peak area for band 1420 cm^{-1}
Y_{SSCHT} is the Chitosan yield
m_{SSCHT} is the Weight of extracted shrimp shell chitosan
m_{SS} is the Weight of the shrimp shell

Preparation of CPS/SSCHT/SOR Bioplastic Film

The bioplastic films were produced according to Tan et al.'s (2022) research design with slight modifications. The mass percent of each component was scaled to a total of 1.5 grams for each run. Distilled water amounting to 12.5 mL and 5 mL of 1% v/v acetic acid were added

to each sample, then heated in a double-boiler set up and mixed until gelatinized. The sample was poured into a 90 mm petri dish mold and dried in a furnace at 30 °C for 12 hours. The CPS/SSCHT/SOR bioplastic films were then characterized by tensile strength, elongation at break, contact angle, and opacity.

Determination of Tensile Strength and Elongation at Break

Mechanical properties of tensile strength and elongation at break were tested based on Flores et al.'s (2024) research design. The films were cut following ASTM D638 protocol before being assessed according to ASTM D882 protocols with a Zwick Roell Z0.5 Universal Testing Machine (Zwick Roell Group, Ulm, Germany) at a load cell of 500 N at room temperature at a 500 mm/min crosshead speed and from the initial 50 mm separation. Each film was tested in triplicates, and the tensile strength and elongation at break for each run were recorded.

Determination of Contact Angle

The contact angle utilizing ASTM D5946 protocols with modifications as per Guzman-Puyol et al.'s (2022) sessile drop method. A puncher was used to obtain small, circular films for testing to ensure a uniform sample size. The contact angle of CPS/SSCHT/SOR bioplastic films was measured by placing the film on a small Petri dish within a lightbox to enhance visual clarity. A syringe was used to deposit a drop of water onto the surface of each film, and the droplets were then photographed. A digital protractor was used to measure the angle of the droplet against the bioplastic surface.

Determination of Opacity

The opacity of the films were determined according to Nigam et al.'s (2021) design. The films were cut to 4 cm. x 1 cm., then tested in triplicates with a UV-VIS Spectrophotometer at 600 nm with a blank cell serving as the reference opacity. Opacity was then calculated using Equation 6.

$$Opacity\ (\%) = \frac{A_{600nm}}{thickness} \times 100 \quad (6)$$

Wherein:
$A_{600\ nm}$ is the Absorbance at 600 nm
Thickness is the Thickness of film (mm)

Characterization of CPS/SSCHT/SOR Bioplastic Film

This method was modeled after Tan et al.'s (2022) design. An FTIR spectrometer was utilized in attenuated total reflectance (ATR) mode and positioned on the film's surface to record the FTIR spectra of the optimized film and determine its chemical bonds and functional groups. The sample was scanned at a frequency range of 4000-450 cm^{-1}. The FTIR spectra was recorded and presented in a line graph, and compared to the spectra of shrimp shell chitosan and cassava peel starch. Thermogravimetric analysis (TGA) was adapted from the study of Mofokeng et al. (2011) with slight modifications. Film weighing 5.086 mg was subjected to the TGA55 thermogravimetric analyzer (TA Instruments, New Castle, DE, USA). Nitrogen was utilized at a sample purge flow rate of 25.01 mL/min and a balance purge flow rate of 40.01 mL/min. The film was equilibrated to 30 °C then heated at a ramp value of 10 °C/min until 600 °C.

Statistical Analysis

JMP 18.1.1. software was utilized for the generation of the 10-point D-Optimal constrained mixture design, analysis of variance (ANOVA), fit modeling, and the generation of response ternary plots based on the calculated prediction formulas. Responses were modeled by Scheffe's Cubic models with Equation 7, wherein y represents the dependent variable, β represents the coefficient of the model, and subscripts 1, 2, and 3 represent shrimp shell chitosan, cassava peel starch, and sorbitol, respectively. The responses were modeled with a significance level of 5% ($p \leq 0.05$).

$$y = \beta_1 x_1 + \beta_2 x_2 + \beta_3 x_3 + \beta_{12} x_1 x_2 + \beta_{13} x_1 x_3 + \beta_{23} x_2 x_3 + \beta_{123} x_1 x_2 x_3 \quad (7)$$

The assumptions for ANOVA were tested using Shapiro-Wilk and Anderson-Darling tests for normality, Levene's test for homogeneity of variance, and independence between the variables. Assumptions for regression analysis were verified using an actual by predicted plot generated by the Scheffé cubic model.

Ethics Statement

The research methods have been designed to address the given research questions. All methods have been reviewed and referenced from relevant studies to ensure the validity, feasibility, and accuracy of the results obtained. All data was diligently recorded and reported with transparency. No data was fabricated, falsified, or plagiarized.

Considering the emphasis on sustainability and food security in this study, only food waste materials were utilized. No edible food materials, namely shrimp meat and cassava flesh, were used or wasted in the experiment. Food materials were either managed by the provider or consumed. Any materials from the experimental methods involved in the research design were discarded accordingly and appropriately.

Result and Discussion

Cassava Peel Starch Extraction and Characterization

The cassava peels collected for starch extraction were initially covered in dirt and other ecological residues due to their contact with soil (see Figure 2a). Proper washing and isolation of the cassava peel cortex were essential to prevent contamination, as insufficient cleaning would result in a grainy brown starch extract. To improve purity, the peels were separated from the dark brown lignified portion, as its presence could introduce impurities and affect the final starch quality (see Figure 2b). Following the blending of these peels, each time the extract was filtered through the cheesecloth, it was noticeably whiter with each filtration compared to its initial beige state. After extraction, the cassava peel starch extract underwent centrifugation to eliminate the remaining residues. After each cycle, the dark sediment that settled on top of the white starch was carefully removed (see Figure 2c). This process was repeated until no visible impurities remained, and the resulting extract was then lyophilized (see Figure 2d), resulting in a cleaner and more refined starch comparable to those that are commercially available

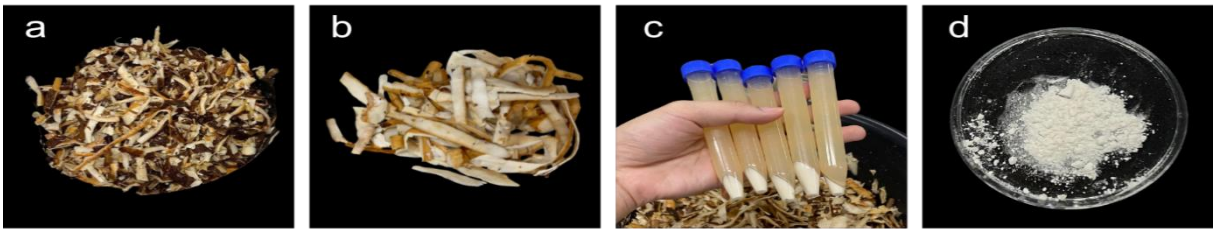

Figure 2. Extraction process of cassava peels

The cassava peel starch extraction process resulted in a 7.90% ± 1.91% dry basis yield, which was approximately 20% greater than the reported yield (6.5%) from the results obtained by Fronza et al. (2022). Cassava peel starch was compared with commercial cassava starch (CCS) as a benchmark in terms of FTIR spectroscopy, as seen in Figure 3.

Identified functional groups and their assigned wavenumbers were collated and summarized in Table 2 for cassava peel starch. The peaks at 1015 cm^{-1} and 1190cm^{-1} for cassava peel starch represent the C—O—H bend and the C—O and C—C stretches of the glucopyranose rings, as corroborated by Thuppahige et al. (2023). These values are similarly matched with CCS at 1012cm^{-1} and 1190cm^{-1}, respectively. The O—H stretch at 3318cm^{-1} represents the intermolecular hydrogen bonding within OH groups (Garces et al., 2021) and glucopyranose rings (Thuppahige et al., 2023). The C—H bond at 2927cm^{-1} is attributed to CH_2 asymmetric aliphatic groups, whereas the presence of water molecules was denoted by the deformation of the O—H bond at 1645cm^{-1} (Thuppahige et al., 2023). The peak at 1502cm^{-1} is associated with the C=C stretching of the aromatic ring of lignin (Widiarto et al., 2017).

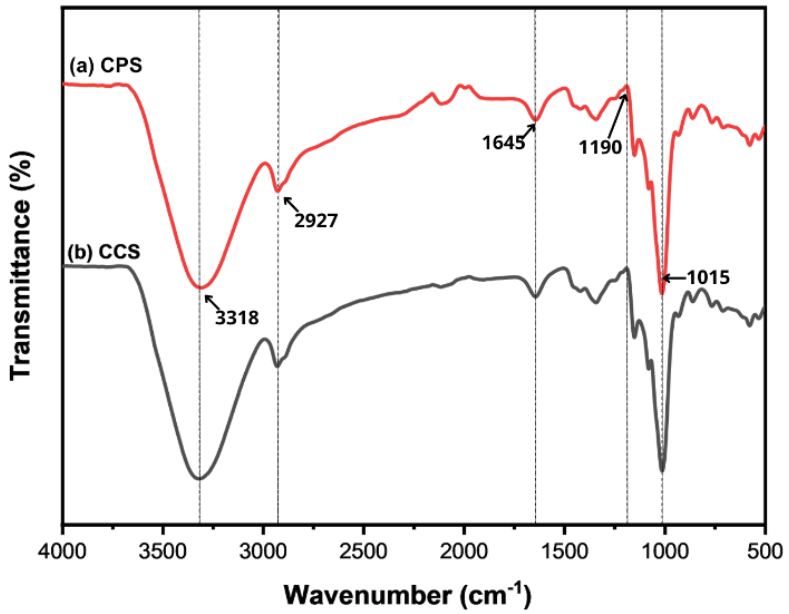

Figure 3. FTIR spectra of (a) cassava peel starch (CPS) and (b) commercial cassava starch (CCS)

Table 2. Wavenumbers and associated functional groups of FTIR spectra of cassava peel starch

Wavenumber (cm^{-1})	Functional group
2926-2927	C—H bond (Abdullah et al., 2018; Fronza et al., 2022; Thuppahige et al., 2023)
1645	O—H bond deformation (Fronza et al., 2022; Thuppahige et al., 2023)
1012-1015	C—O—H bend (Lomelí-Ramírez et al., 2014; Thuppahige et al., 2023)
1190	C—O stretch (Abdullah et al., 2018; Thuppahige et al., 2023)
1190	C—C stretch (Thuppahige et al., 2023)
1502	C=C stretch (Widiarto et al., 2017)
3310-3318	O—H stretch (Lomelí-Ramírez et al., 2014; Thuppahige et al., 2023)

Extraction and Characterization of Shrimp Shell Chitosan

The stages of chitosan extraction from shrimp shells are shown in Figure 4. Shrimp shells were manually washed and cleaned of residues then dried (see Figure 4a). The resulting chitin post-deproteinization and decalcification as seen in Figure 4b exhibited a tan to brown color. This was improved upon and lightened by means of bleaching, with the result as shown in Figure 4c. The shrimp shell chitosan product (see Figure 4d) exhibited a fine powdery texture with a slightly tan color. The shrimp shell chitosan extraction process resulted in a 6.09% ± 0.61% dry basis yield, around 100% lower than the results obtained by Aberoumand and Chabavi (2024) (14.72% ± 0.57% & 12.03% ± 0.46%) and Varun et al. (2017) (13.96%). This reduced yield could be due to the utilization of green Gly/5%CA solvent in deproteinization and decalcification for chitin as opposed to strong chemicals such as 3M HCl (Aberoumand & Chabavi, 2024) and 2N HCl acid (Varun et al., 2017). Extracted shrimp shell chitosan had an 80.22% degree of deacetylation, resulting in a medium deacetylation degree standard classification, and can thereby be used for industrial products (Li et al. 2020).

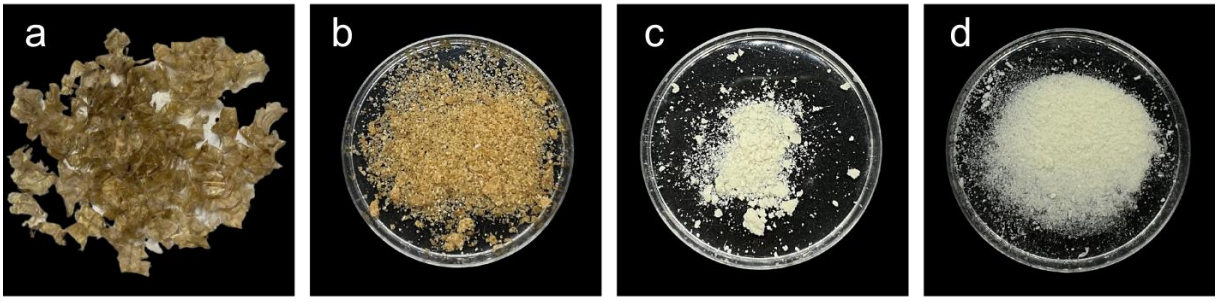

Figure 4. Extraction stages of shrimp shells

FTIR spectrographs were generated for shrimp shell chitosan, shrimp shell chitin, and shrimp shells, as shown in Figure 5. The assigned wave bands for shrimp shell chitosan are summarized in Table 3. The first distinct peak was found at 3336 cm^{-1}, which is associated with O-H & N-H stretching, and at 2886 cm-1, which indicates C-H stretching typical of polysaccharide spectra. Moreover, weak amide peaks were found at 1622 cm^{-1} (Amide I) and 1521 cm^{-1} (Amide II). The diminished intensity of these amide bands, compared to the graph of chitin and shrimp shell, supports the high deacetylation degree, reflecting reduced acetyl group retention in the extracted chitosan. These peaks were consistent with those found and discussed by Elhaes et al. (2024). The absence of a peak at 1540 cm^{-1}, where the Amide II band typically appears in chitosan samples, suggest successful deproteinization. However, the presence of a weak peak at 1521 cm^{-1}, an amide group-associated region, indicates that while most proteins were removed, minor residual protein content may still be present (Vallejo-Dominguez et al., 2021).

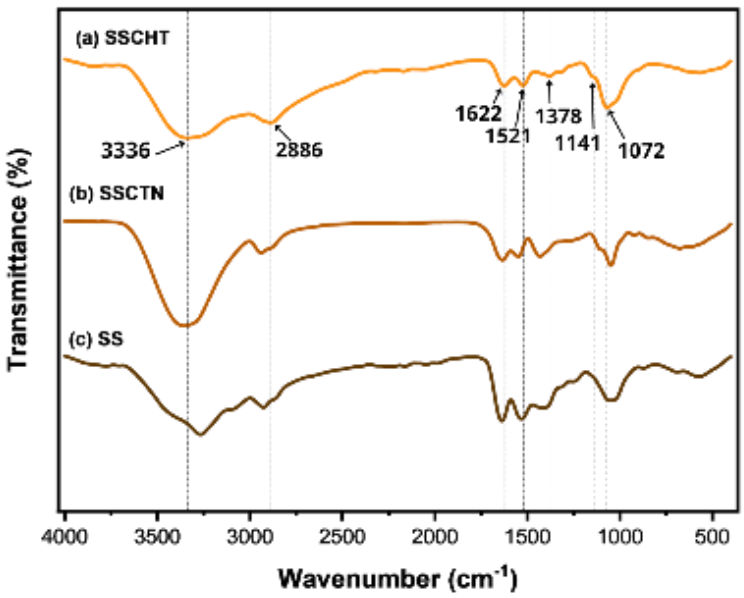

Figure 5. FTIR spectra of (a) shrimp shell chitosan (SSCHT), (b) shrimp shell chitin (SSCTN), and (c) shrimp shell (SS)

Table 3. Wavenumbers and associated functional groups of FTIR spectra of shrimp shell chitosan.

Wavenumber (cm^{-1})	Functional group
3336	OH and NH stretching (Elhaes et al., 2024)
2886	CH stretching (Elhaes et al., 2024)
1622	C–N–H, amide I (Elhaes et al., 2024)
1521	O=C–NH_2, amide II (Elhaes et al., 2024)
1378	CH_3 bending (Elhaes et al., 2024)

Preparation of CPS/SSCHT/SOR Bioplastic Films

An overview of prepared bioplastics was collated and presented in Figure 6, with each number corresponding to their respective run. The produced films presented a glossy finish with BP-2, BP-5, and BP-9 exhibiting minimal air bubbles. All three films had varying concentrations of each component, implying that component concentration may not have been a major reason for the difference in film consistency. Rather, this difference could be attributed to the casting method, raising the need for adjustment to address the presence of bubbles, such as the utilization of ultrasonication. The real concentrations of each run and their responses in terms of tensile strength, elongation at break, contact angle, and opacity are summarized in Table 4.

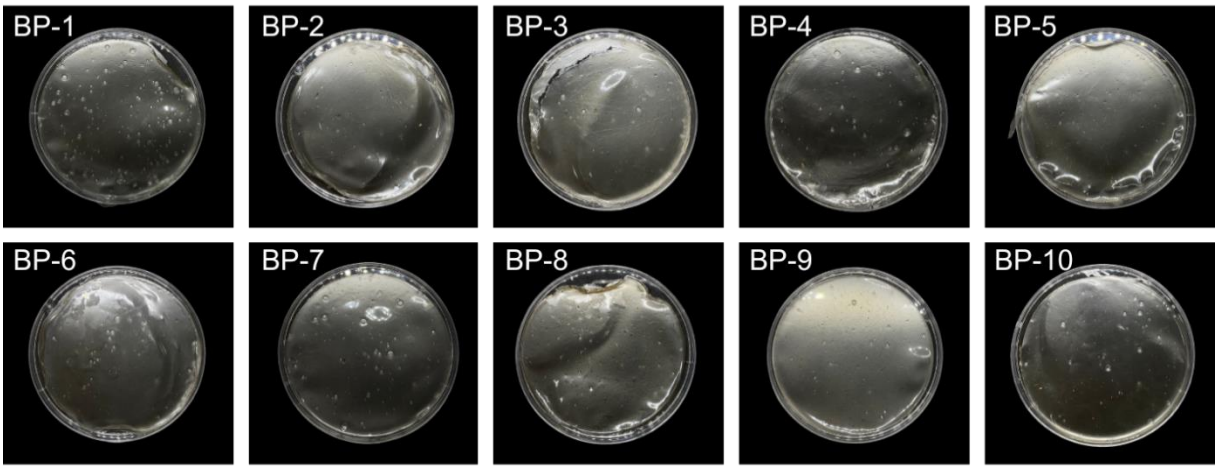

Figure 6. Produced CPS/SSCHT/SOR films classified by run number

Table 4. Responses of dependent variables tensile strength, elongation at break, contact angle, and opacity for films of varying cassava peel starch (CPS), shrimp shell chitosan (SSCHT), and sorbitol (SOR) composition

Run number	Real concentrations			Responses			
	CPS (%)	SSCHT (%)	SOR (%)	Tensile Strength (MPa)	Elongation at Break (%)	Contact Angle (°)	Opacity (%)
BP-1	77	5	18	44.8 ± 11.2	1.696 ± 0.27	55.33 ± 4.16	2.05 ± 0.19
BP-2	70	5	25	30.4 ± 7.10	1.754 ± 0.18	71.67 ± 9.07	2.94 ± 0.25
BP-3	75	0	25	32.5 ± 1.55	1.871 ± 0.10	65.00 ± 10.44	2.76 ± 0.40
BP-4	82	0	18	37.1 ± 10.7	1.696 ± 0.27	39.33 ± 3.21	2.06 ± 0.35
BP-5	77	5	18	45.6 ± 7.04	1.930 ± 0.18	66.67 ± 2.89	2.95 ± 0.25
BP-6	76	2.5	21.5	35.3 ± 3.90	1.813 ± 0.20	52.67 ± 11.37	2.52 ± 0.14
BP-7	76	2.5	21.5	32.0 ± 2.24	1.988 ± 0.56	62.00 ± 1.73	2.42 ± 0.10

Run number	Real concentrations			Responses			
	CPS (%)	SSCHT (%)	SOR (%)	Tensile Strength (MPa)	Elongation at Break (%)	Contact Angle (°)	Opacity (%)
BP-8	70	5	25	22.1 ± 2.66	2.398 ± 0.54	87.00 ± 2.65	2.72 ± 0.36
BP-9	82	0	18	32.8 ± 3.38	1.930 ± 0.18	39.67 ± 4.73	2.28 ± 0.05
BP-10	75	0	25	31.5 ± 3.64	1.871 ± 0.27	36.67 ± 3.06	1.60 ± 0.12

Effect of Mixture Composition on Tensile Strength

The histogram shows a bell-shaped curve, and the points of the quantile (Q-Q) plot fall approximately on the straight line as shown in Figure 7. Additionally, the Shapiro-Wilk test also revealed a non-significant p-value (p = 0.3292) along with the Anderson-Darling test (p = 0.2008). This entails a normal distribution for tensile strength against the composition of the CPS/SSCHT/SOR film. Levene's test confirmed homogeneity of variances, revealing a p-value greater than significance level (p = 1.0000). The run chart generated in JMP showed no evident patterns or trends over time, supporting the assumption of independence.

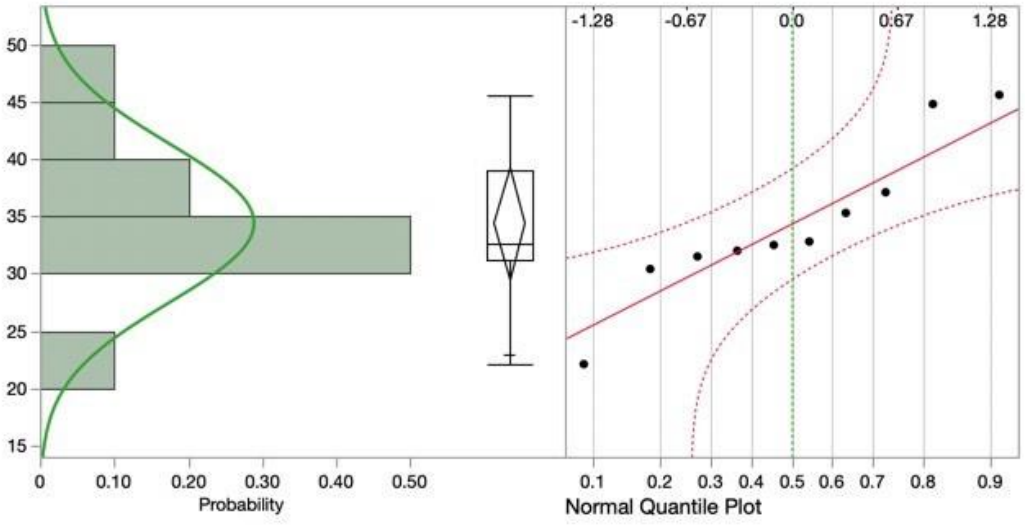

Figure 7. Graph of histogram and quantile plot of tensile strength

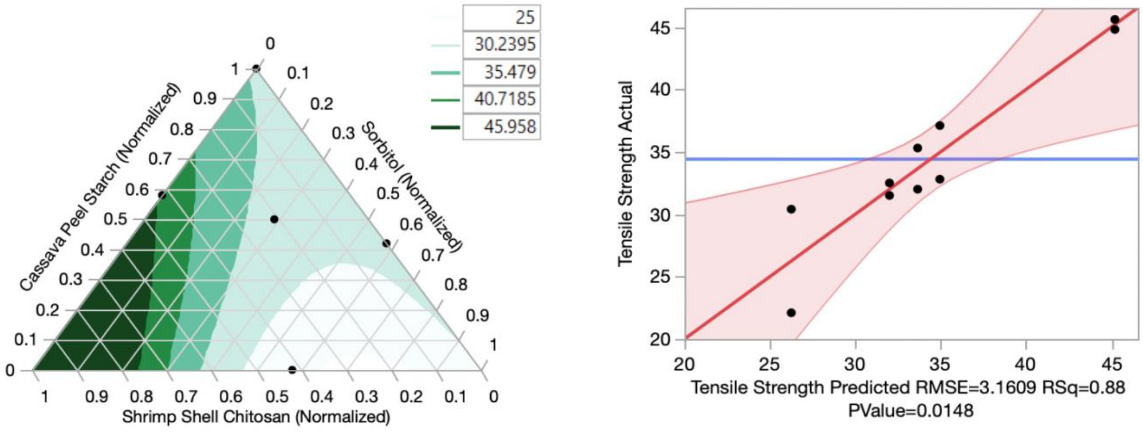

(a) (b)

Figure 8. Plot of (a) ternary diagram showing the predicted tensile strength based on mixture composition and (b) actual tensile strength against predicted tensile strength

The tensile strength prediction model generated was significant (p = 0.0148), which confirms that the regression is meaningful, with R^2 = 0.88 as seen in Figure 8b. The high R^2 is attributed to the combined effects of all three components. Additionally, the actual by predicted plot as seen in Figure 8b shows that the plots are scattered with no discernible pattern around the 45-degree line, which entails the components, and the tensile strength results are non-linear, meaning the result of the tensile strength varies with the values of the components. Moreover, both cassava peel starch (p = 0.0001) and sorbitol (p = 0.0008) had a significant effect on tensile strength as seen in Table 5, which could be attributed to the linear chains formed in starch amylose (Domene-López et al., 2019), and the bonding of hydroxyl groups (Fatima et al., 2024), whereas sorbitol's reduced yet positive impact could be due to its nature as a plasticizer, disrupting chains and improving flexibility to withstand stress, but may interfere with the film's structural integrity (Domene-López et al., 2019). However, of the three components, shrimp shell chitosan concentration had the largest magnitude despite being insignificant (p = 0.0877). Runs with increased concentrations of cassava peel starch and shrimp shell chitosan resulted in the highest tensile strength, as observed in films BP-1 and BP-5 in Table 4. This increase could be attributed to –OH groups exposed due to the gelatinization of starch in bioplastic double-boiler mixing undergoing hydrogen bonding with $–NH_2$ groups in chitosan (Pelissari et al., 2012).

Table 5. Regression coefficients and parameter estimates of tensile strength in terms of shrimp shell chitosan, cassava peel starch, and sorbitol

Parameters	β_1	β_2	β_3	β_{12}	β_{13}	β_{23}	β_{123}
Parameter Estimates	71.85	34.95	29.86	-21.54	-87.22	-	-
p-value	0.0877	<0.0001	0.0008	0.7194	0.2030	-	-

Pelissari et al. (2012) utilized a similar constrained mixture design but with glycerol in place of sorbitol and extrusion instead of casting, obtaining a range of 0.99 MPa ± 0.05 MPa to 2.71 MPa ± 0.25 MPa compared to the results achieved in this study. Although Pelissari et al. (2012) stated that the reduced tensile strength was due to a lesser concentration of chitosan, Shen et al. (2010) utilized a similar concentration of chitosan to rice starch yet achieved a greater tensile strength. Whereas Pelissari et al. (2012) utilized extrusion processes, Shen et al. (2010) formed films by means of casting, which may have contributed to the difference in tensile strength. Yan et al. (2012) conducted a study on the effects of extrusion on starch-based films and found that treated films resulted in poorer tensile strength due to the high temperature and strong shear treatment of the process. Thus, the film formation process, namely between casting and extrusion, is a factor to consider for tensile strength.

Table 6. ANOVA of tensile strength

Source	DF	Sum of squares	Mean of squares	F ratio	Prob > F
Model	4	379.37	94.83	9.49	0.0148*
Error	5	49.95	9.99	-	-
U. Total	9	429.32	-	-	-

Effect of Mixture Composition on Elongation at Break

The histogram shows a central peak but also unevenness among the distribution, increasing the likelihood of minor deviations from complete normality. Despite this, the points of the quantile (Q-Q) plot fall approximately on the straight line as shown in Figure 9. Additionally, the Shapiro-Wilk test also revealed a significant p-value (p = 0.0241) along with the Anderson-Darling test (p = 0.0472). This entails that the data deviates

from normality for elongation at break against the composition of the CPS/SSCHT/SOR film. The Levene's test confirmed homogeneity of variances revealing a p-value greater than significance level (p = 1.0000). The run chart generated in JMP showed no evident patterns or trends over time, supporting the assumption of independence.

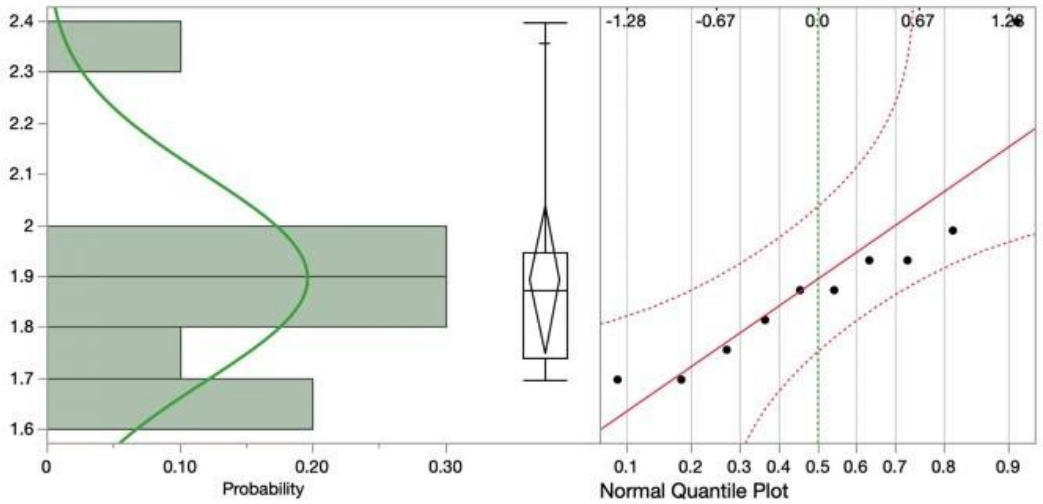

Figure 9. Graph of histogram and quantile plot for elongation of break

Maximum elongation at break was achieved at 2.398% ± 0.54% in BP-8 with maximum sorbitol and minimum cassava peel starch, the same film that exhibited the poorest tensile strength. Minimum elongation at break was achieved at 22.1 MPa ± 2.66 MPa in BP-1 and BP-4. The overall low elongation at break response suggests that the synthesized CPS/SSCHT/SOR films were very inelastic and unfit for plastic applications similar to cling wrap. Tensile strength and elongation at break must be discussed hand in hand, as their individual responses are often connected and inversely proportional. Tan et al. (2022) tested films with constant starch concentrations but varying glycerol loading, which found that increasing glycerol concentration resulted in greater elongation at break but reduced tensile strength due to the weakening of the polymer matrix while allowing glycerol molecules to disrupt amylose-amylopectin chains. This phenomenon is similarly observed in BP-1 and BP-8 from Table 4, which exhibited high tensile strength but poor elongation at break and vice versa, respectively.

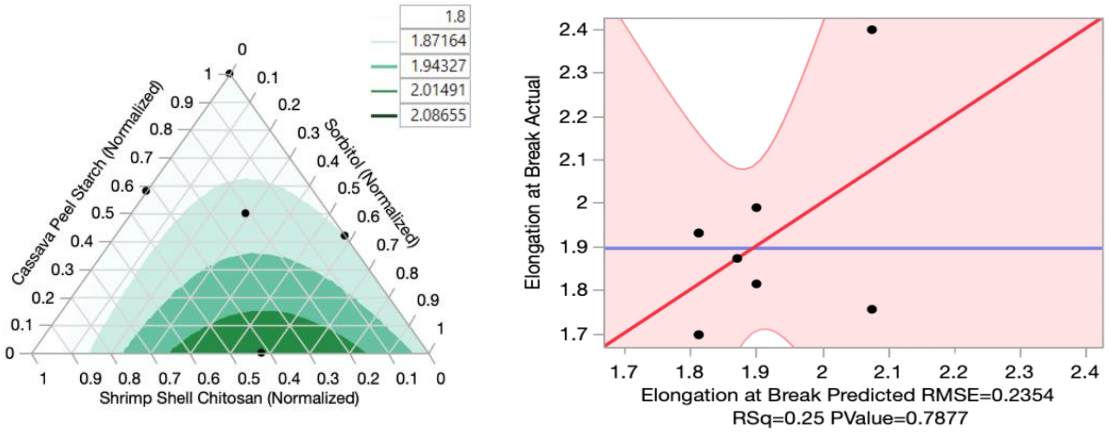

(a) (b)

Figure 10. Plot of (a) ternary diagram showing the predicted elongation at break based on mixture composition and (b) actual elongation at break against predicted elongation at break

The elongation at break response ternary plot as shown in Figure 10a. revealed that maximum elongation at break was achieved with reduced shrimp shell chitosan, moderate sorbitol, and minimal cassava peel starch. Furthermore, the vertical contours illustrate the influence of cassava peel starch concentration on elongation at break, wherein increasing cassava peel starch led to a reduced response. The contours in Figure 10a were darker in regions that were lighter in Figure 9a., further highlighting the negatively linear relationship between tensile strength and elongation at break.

The elongation at break model had a high variability (p = 0.7877), yielding an R^2 value of 0.25 as seen in Figure 10b. This indicates that the elongation at break response cannot be consistently predicted based on component composition. However, despite the overall p-value being insignificant, the parameter estimates of cassava peel starch (p = 0.0001) and sorbitol (p = 0.0017) were both significant factors to the elongation at break response, as seen in Table 7. This could indicate that although the response prediction was unreliable, certain components' concentration could still hold implications with regard to its impact on elongation at break. The results suggest that both cassava peel starch and sorbitol lead to a reduced elongation at break. The intermolecular bonds found within starch allow for greater rigidity (Wang et al., 2018). Although this rigidity could be addressed by the incorporation of a plasticizer like sorbitol, its large molecular weight (182.17 g/mol) and, thereby, molecular mobility increase in the starch matrix (Zahiruddin et al., 2019) and structural similarity with starch glucose units allows for more interactions (Abdollahi Moghaddam et al., 2023). Sorbitol's 6-carbon chain and multiple hydroxyl groups allowed for greater hydrogen bonding with starch, which may have further contributed to the films' inelastic nature.

Table 7. Regression coefficients and parameter estimates of elongation at break in terms of shrimp shell chitosan, cassava peel starch, and sorbitol

Parameters	β_1	β_2	β_3	β_{12}	β_{13}	β_{23}	β_{123}
Parameter Estimates	1.72	1.81	1.91	0.17	1.01	-	-
p-value	0.5269	0.0001	0.0017	0.9702	0.8295	-	-

Sorbitol's impact on the elongation at break dependent variable of the film is highlighted when contrasted with glycerol. Due to its smaller molecular weight (92.09 g/mol) and 3-carbon chain with fewer hydroxyl groups (Lerbret et al., 2009), glycerol is able to incorporate into polymer chains more effectively, promoting flexibility (Ballesteros-Mártinez et al., 2020). As such, the utilization of sorbitol leads to greater tensile strength but reduced elongation at break, whereas glycerol produces greater elasticity but weaker films, as supported by the observations of Abdollahi Moghaddam et al. (2023), Ooi et al. (2012), and Zahiruddin et al. (2019).

Table 8. Regression coefficients and parameter estimates of elongation at break in terms of shrimp shell chitosan, cassava peel starch, and sorbitol

Parameters	β_1	β_2	β_3	β_{12}	β_{13}	β_{23}	β_{123}
Parameter Estimates	1.72	1.81	1.91	0.17	1.01	-	-
p-value	0.5269	0.0001	0.0017	0.9702	0.8295	-	-

Sorbitol's impact on the elongation at break dependent variable of the film is highlighted when contrasted with glycerol. Due to its smaller molecular weight (92.09 g/mol) and 3-carbon chain with fewer hydroxyl groups (Lerbret et al., 2009), glycerol is able to incorporate into polymer chains more effectively, promoting flexibility (Ballesteros-Mártinez et al., 2020). As such, the utilization of sorbitol leads to greater tensile strength but reduced

elongation at break, whereas glycerol produces greater elasticity but weaker films, as supported by the observations of Abdollahi Moghaddam et al. (2023), Ooi et al. (2012), and Zahiruddin et al. (2019).

Table 8. ANOVA of elongation at break

Source	DF	Sum of squares	Mean of squares	F ratio	Prob > F
Model	4	0.093	0.023	0.42	0.7877
Error	5	0.27	0.055	-	-
U. Total	9	0.37	-	-	-

Effect of Mixture Composition on Contact Angle

The histogram shows a central peak but also unevenness among the distribution increasing the likelihood of minor deviations from complete normality. Despite this, the points of the quantile (Q-Q) plot fall approximately on the straight line as shown in Figure 11. Additionally, the Shapiro-Wilk test also revealed a non-significant p-value (p = 0.6301) along with the Anderson-Darling test (p = 0.6888). This entails a normal distribution for contact angle against the composition of the CPS/SSCHT/SOR film. The Levene's test confirmed homogeneity of variances revealing a p-value greater than significance level (p = 1.0000). The run chart generated in JMP showed no evident patterns or trends over time, supporting the assumption of independence.

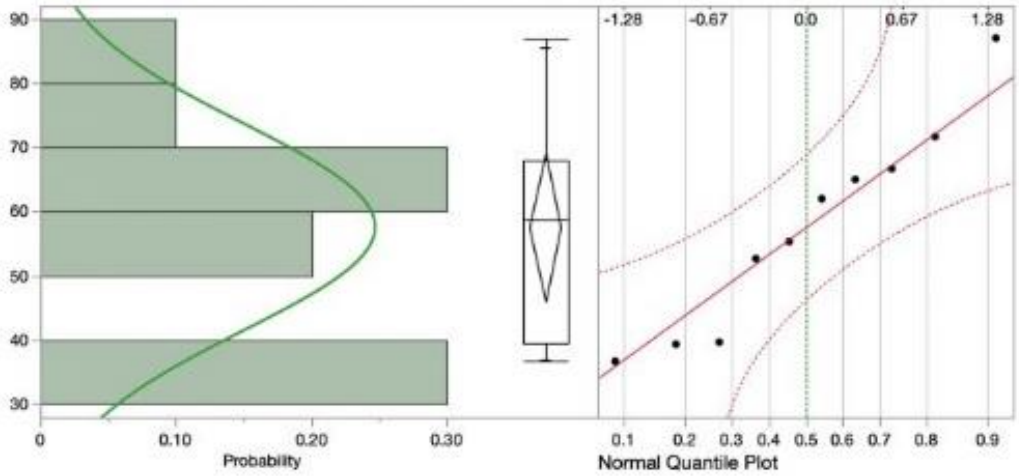

Figure 11. Graph of (a) histogram and (b) quantile plot of contact angle

Maximum contact angle was achieved at 87.00° ± 2.65° in BP-8 with maximum sorbitol, maximum shrimp shell chitosan, and minimum cassava peel starch, the same film that exhibited the highest elongation at break. Minimum contact angle was achieved at 36.67° ± 3.06° in BP-10 with maximum sorbitol, no shrimp shell chitosan, and a moderate amount of cassava peel starch. The overall contact angle range across all runs categorized the films as hydrophilic ($\theta \leq 90°$) materials (Jaderi et al., 2023). The effect of component concentration is further highlighted in Figure 13a, wherein value larger than 80.93° contact angle was achieved with minimal cassava peel starch, minimal to moderate sorbitol, and maximum shrimp shell chitosan. The orientation and direction of the contours in Figure 13a suggest that sorbitol had a reduced impact on contact angle, which can be similarly observed in how both minimum and maximum contact angle were achieved with 25% sorbitol. Albar et al. (2024) reported that contact angle improved due to the incorporation of amino group $-NH_2$ in chitosan, increasing hydrophobicity.

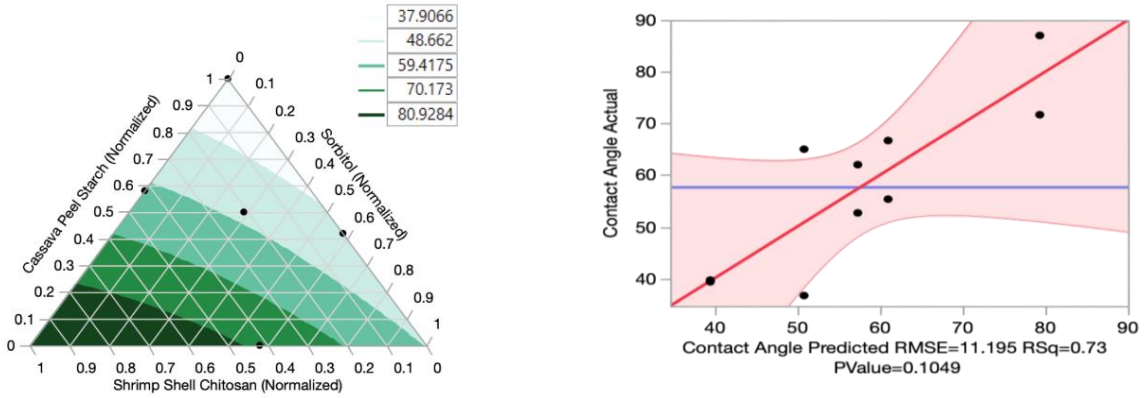

(a) (b)

Figure 12. Plot of (a) ternary diagram showing the predicted contact angle based on mixture composition and (b) actual contact angle against predicted contact angle

The model generated for the contact angle response revealed a high variability (p = 0.1049), indicating that the relationship of the components and contact angle is not significantly strong in the model, but still provides a high R^2 value of 0.73, as seen in Figure 12b. Additionally, the predicted by actual plot as seen in Figure 13b show no true pattern along the 45-degree line entailing that although the model has an insignificant p-value it still shows a non-linear relationship between the components and contact angle results. While the model was unpredictable, parameter estimates cassava peel starch (p = 0.0041) and sorbitol (p = 0.0104) as seen in Table 9 were significant, which may be attributed to starch's numerous hydroxyl groups (Wang et al., 2020) and sorbitol's ability to reduce internal hydrogen bonds (Arief et al., 2021) and thereby increased interaction with external water molecules (Chen et al., 2019). Although the parameters for shrimp shell chitosan were found to be too inconsistent to be reliable, its high magnitude suggests its impact in promoting hydrophobicity in the developed films. Although not inherently hydrophobic (Wang et al., 2023), chitosan's compatibility with the starch matrix (Kusumaningrum et al., 2023) allowed for greater hydrogen bonding between the two components (Rajesh, 2023) while minimizing hydrophilic regions for external water molecule penetration.

Table 9. Regression coefficients and parameter estimates of contact angle in terms of shrimp shell chitosan, cassava peel starch, and sorbitol

Parameters	β_1	β_2	β_3	β_{12}	β_{13}	β_{23}	β_{123}
Parameter Estimates	95.06	39.50	59.04	-7.54	21.20	-	-
p-value	0.4647	0.0041	0.0104	0.9715	0.9239	-	-

Table 10. ANOVA of contact angle

Source	DF	Sum of squares	Mean of squares	F ratio	Prob > F
Model	4	1714.83	428.70	3.42	0.1049
Error	5	626.67	125.33	-	-
U. Total	9	2341.51	-	-	-

Effect of Mixture Composition on Opacity

The histogram as seen in Figure 13a shows a central peak but also unevenness among the distribution increasing the likelihood of minor deviations from complete normality. Despite this, the points of the quantile (Q-Q) plot fall

approximately on the straight line. Additionally, the Shapiro-Wilk test also revealed a non-significant p-value (p = 0.5901) along with the Anderson-Darling test (p = 0.7356). This entails a normal distribution for contact angle against the composition of the CPS/SSCHT/SOR film. For homogeneity of variance, the Levene's test results in a dot wherein the p-value is very small and often less than 0.001 indicating a statistically significant difference in variances between groups. The run chart generated in JMP showed no evident patterns or trend over time, supporting the assumption of independence.

As shown in Figure 13b, minimum opacity was achieved at 1.60% ± 0.12% in BP-10 with maximum sorbitol, no shrimp shell chitosan, and a moderate amount of cassava peel starch, the same film with the poorest hydrophobicity. Maximum opacity was achieved at 2.95% ± 0.25% in BP-5 with minimum sorbitol, maximum shrimp shell chitosan, and moderate cassava peel starch. The produced films were more transparent than those designed by Oluwasina et al. (2024), which yielded an opacity ranging from 14.78-38.64%.

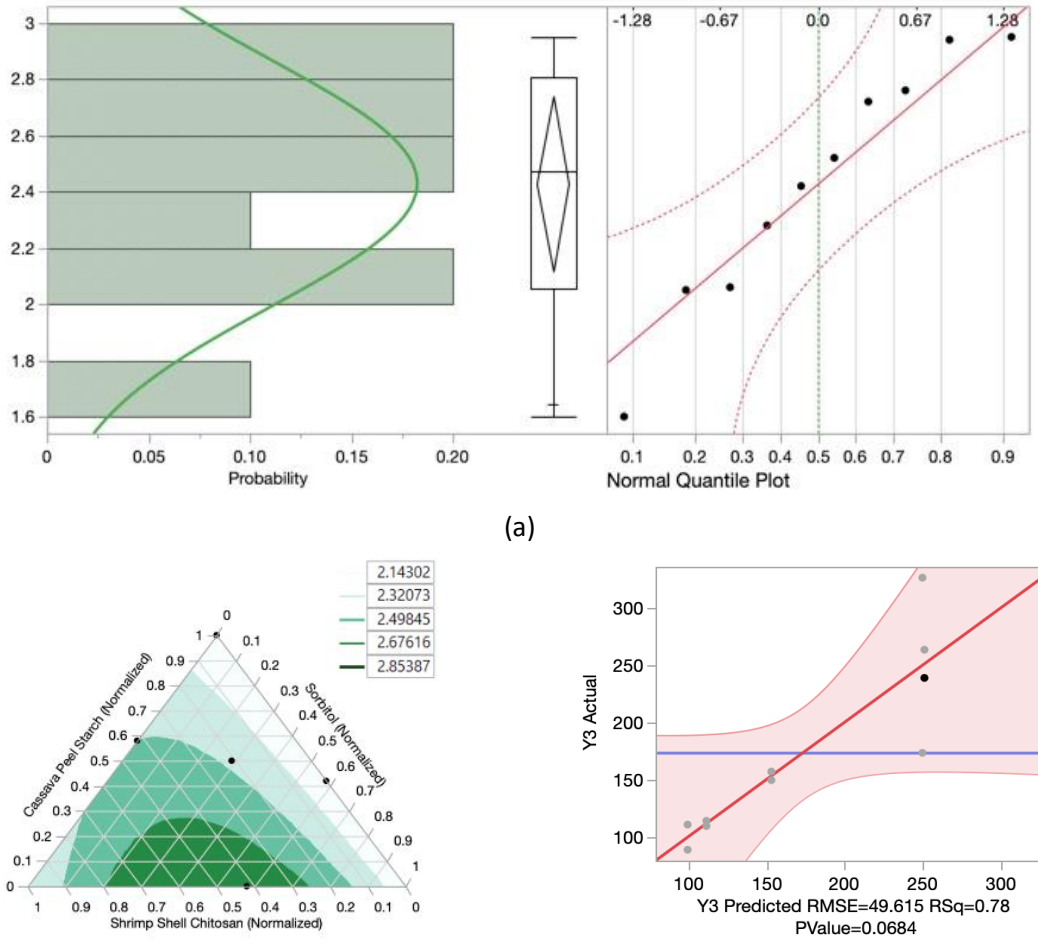

Figure 13. Graph of (a) histogram, quantile plot, (b) ternary diagram showing the predicted opacity based on mixture composition and (c) plot of actual opacity against predicted opacity

The films' overall high transparency implies its viability as plastic packaging without hindering the visibility of the product, which is one of the most important implications of a film's opacity (Oluwasina et al., 2024). It is also worth noting that the contours seen in Figure 13a lighten as cassava peel starch increased, which may be due to starch gelatinization and retrogradation. As the film solution is heated,

starch swells and bursts, undergoing gelatinization in which amylose cools to an opaque gel while amylopectin results in a fluid, translucent paste (Pither, 2003). Bashir and Aggarwal (2019) further explained that swollen starch granules refract light, impacting light transmittance and thereby transparency.

The opacity model exhibited a high variability (p = 0.6483), with an R^2 value of 0.34, as seen in Figure 13c. Although the model provides an insignificant p-value and a weak R^2 value, the predicted by actual plot as seen in Figure 13c shows that the relationship between components and opacity values is non-linear meaning the value of the components still affect the results of opacity. Additionally, both parameter estimates for cassava peel starch (p = 0.0013) and sorbitol (p = 0.0178) as seen in Table 11 were significant, which indicates that film opacity may be impacted due to starch's larger particle size (Oluwasina et al., 2021) and retrogradation, as well as sorbitol's nature as a plasticizer to increase transparency (Mohammed et al., 2023). However, shrimp shell chitosan had the highest magnitude in terms of parameter estimates despite being insignificant (p = 0.6174). Although an increase in chitosan was reported to result in a decrease in opacity due to its similarity in form to white powder (Apriliyani et al., 2020), the contours, as seen in Figure 13b, highlight that minimal opacity was achieved with minimal to no shrimp shell chitosan. This could be attributed to its hydrophilic nature and interaction with water molecules, thereby reducing transmittance in the UV region, as corroborated by Cazón et al. (2020).

Table 11. Regression coefficients and parameter estimates of opacity in terms of shrimp shell chitosan, cassava peel starch, and sorbitol

Parameters	β_1	β_2	β_3	β_{12}	β_{13}	β_{23}	β_{123}
Parameter Estimates	2.30	2.17	2.19	1.11	2.43	0	0
***p*-value**	0.6717	0.0013	0.0178	0.9014	0.7957	-	-

Table 12. ANOVA of opacity

Source	**DF**	**Sum of squares**	**Mean of squares**	**F ratio**	**Prob > F**
Model	4	0.59	0.14	0.65	0.6483
Error	5	1.31	0.22	-	-
U. Total	9	1.72	-	-	-

Characterization of CPS/SSCHT/SOR Bioplastic Films

The FTIR spectra for the CPS/SSCHT/SOR film alongside sorbitol, shrimp shell chitosan and cassava peel starch with its corresponding wavenumbers is shown in Figure 14. Functional groups showed a broad peak at about 3336 cm^{-1} which indicates a large number of hydroxyl groups, which was ascribed to –OH stretching vibration (Preethi et al., 2024). The characteristic peaks of inter- and intramolecular hydrogen bonds in starch and chitosan were shifted, revealing the formation of intermolecular hydrogen bonds between starch and chitosan (Tan et al., 2022). Aguilar et al. (2019) mentioned the highest point at the monosaccharide's internal C–H vibrations are represented by approximately 2924 cm^{-1}. Furthermore, at 1638 cm^{-1}, there was a little peak caused by the C=O (Amin et al., 2019). Moreover, the decrease at approximately 1015 cm^{-1} represented by the greatest signal due to C-O vibration (Aguilar et al., 2019). Furthermore, Sangian et al. (2021) entails that the C-C, C-O, C-O (ester), and C-O-H (carbonic acid) bonds emerged at energy bands between 1114 cm^{-1}, which was roughly equivalent to current spectra in the range of 1050 to 1300 cm^{-1}. The absorbance with wavelengths between 580 and 706 cm-1 was typical of the C-O (ester group), which was a sign of the group's capacity to break down. The bonds also are hydrophilic groups wherein water can cause bacteria to enter the bioplastic matrix for degrading (Sangian et al., 2021).

Thermogravimetric analysis was performed to analyze the rate of weight change as a function of temperature including weight or mass changes (growth or loss). This process involves various phenomena, such as weight loss and decomposition, which occur due to the breaking up of chemical bonds. Additionally, evaporation takes place when temperatures rise, causing the loss of volatile components (TA Instruments, 2025). The plot of weight loss against temperature and the derivative is shown in Figure 15.

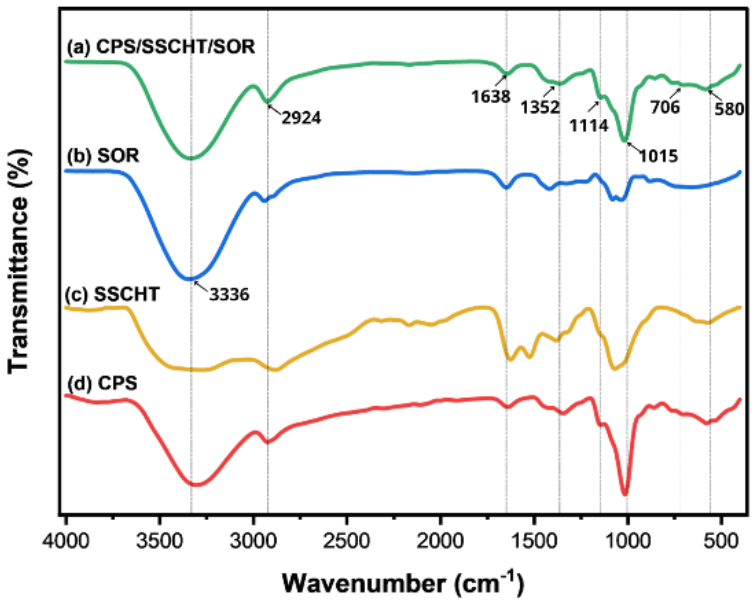

Figure 14. FTIR spectra of (a) CPS/SSCHT/SOR film (CPS/SSCHT/SOR), (b) sorbitol (SOR), (c) shrimp shell chitosan (SSCHT), and (d) cassava peel starch (CPS)

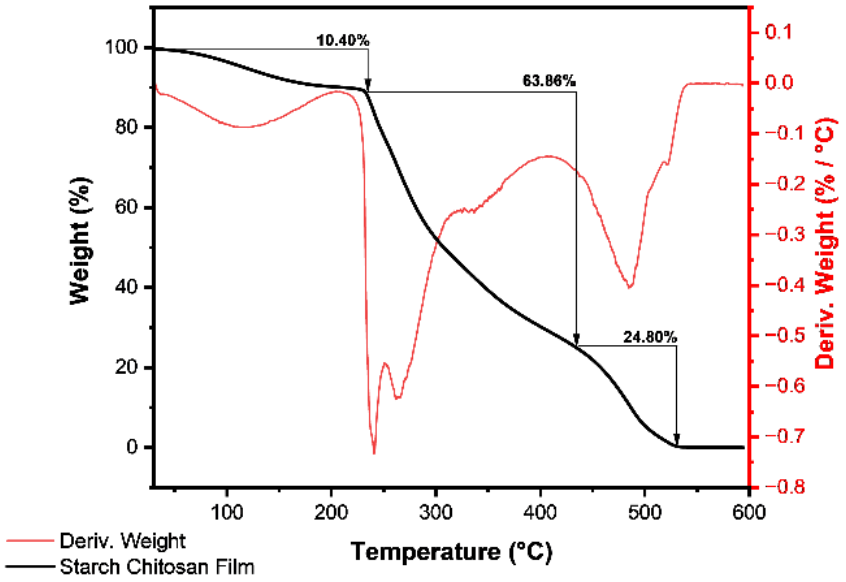

Figure 15. Thermogravimetric analysis thermogram of CPS/SSCHT/SOR bioplastic film showing the weight loss percentage and derivative weight as a function of temperature

In Figure 15, three significant weight losses occurred in response to the temperature changes up to 600 °C. At ~ 60 °C to ~240 °C, there was a 10.40% decrease in weight indicating its first weight loss. Tan et al. (2022) mentioned that the weight loss between 30 °C and

100 °C, was linked to the evaporation of free water. Moreover, the evaporation of moisture from the bioplastic films was the cause of the weight loss which occurred between approximately 100 °C and 200 °C. According to the earlier study, the breakdown of two pectin-based bioplastics (pectin/TA & pectin/CA) takes place between 206 °C and 235 °C and is caused by the scission of saccharide rings in the biopolymer backbone (Tan et al., 2022). This initial weight loss is similar to Feky et al.'s (2024) study where it was visible on the extracted chitosan curve between 50 and 400 °C where in its first stage resulted in about 10.9% weight loss that happened between 50 and 100 °C as a result of the loss of water molecules. The second weight loss that occurred, which was 63.86% at ~240 °C to ~440 °C may be caused by the chitosan's principal deterioration (Feky et al., 2024). The deterioration caused by the depolymerization of composite films and the breakdown of polysaccharides in the temperature range of 337°C to 370 °C may be responsible for the largest mass drop at 265°C to 350 °C which showed that after being heated to 400 °C (Arooj et al., 2023).The third decrease at ~440°C to ~540 °C was due to thermal degradation, which resulted in a 24.80% weight loss. Additionally, there are two mass phases in the TGA analysis of the film sample: thermal deterioration and thermal decomposition which happens at 450 °C (Feky et al., 2024).

In summary, the research explores the viability of valorizing food waste materials and by-products of food processing into materials for bioplastic production. While previous researchers have developed starch/chitosan bioplastic films, these studies commonly utilized commercial or laboratory-grade materials. The extraction, characterization, and utilization of starch and chitosan derived from cassava peel and shrimp shells, respectively, in the development of bioplastic food packaging films would help justify the feasibility and potential of food waste as bioplastic materials. The results of this study could simultaneously address both food waste and plastic waste, two primary concerns of Sustainable Development Goal (SDG) 12, Responsible Consumption and Production.

Conclusion and Recommendations

This study found that the valorization of food waste for the extraction of shrimp shell chitosan and cassava peel starch in the production of a CPS/SSCHT/SOR bioplastic film holds great potential as a sustainable solution to both food waste and plastic waste. The valorization of cassava peels and shrimp shells resulted in good-quality biopolymer materials, namely starch and chitosan, respectively. The optimal film achieved tensile strength of 45.6 MPa ± 7.04 MPa and opacity of 2.95% ± 0.25% in BP-5. The produced films exhibited good tensile strength and transparency, which holds the potential for dry, hard packaging applications. However, the low elongation at break and hydrophilicity as denoted by its contact angle suggests that further adjustments should be made to rectify this, be it by modification or substitution of plasticizer to promote hydrophobicity

References

Abel, O. M., Chinelo, A. S., & Chidioka, N. R. (2021). Enhancing cassava peels starch as feedstock for biodegradable plastic. Journal of Material Environmental Science, 12(2), 169-182. https://www.jmaterenvironsci.com/Document/vol12/vol12_N2/JMES-2021-12016-Abel.pdf

Abdollahi Moghaddam, M. R., Hesarinejad, M. A., & Javidi, F. (2023). Effect of the sorbitol to glycerol weight ratio and sugarcane bagasse concentration on the physicomechanical properties of wheat starch-based biocomposite. Chemical and Biological Technologies in Agriculture, 10(1), 131. https://doi.org/10.1186/s40538-023-00504-6

Abdullah, A. H. D., Chalimah, S., Primadona, I., & Hanantyo, M. H. G. (2018, June). Physical and chemical properties of corn, cassava, and potato starchs. IOP Conference Series: Earth and Environmental Science, 160, 012003. https://doi.org/10.1088/1755-1315/160/1/012003

Aberoumand, A., & Chabavi, M. (2024). Extraction and quality control of chitin and chitosan from shrimp (vanami) litophenause vanamei shells wastes. Natural Product

Communications, 19(10). https://doi.org/1934578X241291383

Aguilar, N. M., Arteaga-Cardona, F., De Anda Reyes, M., Gervacio-Arciniega, J., & Salazar-Kuri, U. (2019). Magnetic bioplastics based on isolated cellulose from cotton and sugarcane bagasse. Materials Chemistry and Physics, 238, 121921. https://doi.org/10.1016/j.matchemphys.2019.121921

Albar, N., Anuar, S. T., Azmi, A. A., Soh, S. K. C., Bhubalan, K., Ibrahim, Y. S., Khalik, W. M. A. W. M., Abdullah, N. S., & Yahya, N. K. E. (2025). Chemical, Mechanical, and Wettability Properties of Bioplastic Material from Manihot esculenta Cassava–Chitosan Blends as Plastic Alternative. Starch-Stärke, 77(1), 2300278. https://doi.org/10.1002/star.202300278

Amin, M. R., Chowdhury, M. A., & Kowser, M. A. (2019). Characterization and performance analysis of composite bioplastics synthesized using titanium dioxide nanoparticles with corn starch. Heliyon, 5(8). https://doi.org/10.1016/j.heliyon.2019.e02009

Apriliyani, M. W., Purwadi, P., Manab, A., W Apriliyanti, M., & D Ikhwan, A. (2020). Characteristics of moisture content, swelling, opacity and transparency with addition chitosan as edible films/coating base on casein. Advance Journal of Food Science and Technology, 18(1), 9-14. http://doi.org/10.19026/ajfst.18.6041

Arooj, A., Khan, M., & Munawar, K. S. (2023). Preparation and physicochemical characterization of starch/pectin and chitosan blend bioplastic films as future food packaging materials. Journal of Environmental Chemical Engineering, 12(1), 111825. https://doi.org/10.1016/j.jece.2023.111825

Arief, M. D., Mubarak, A. S., & Pujiastuti, D. Y. (2021). The concentration of sorbitol on bioplastic cellulose based carrageenan waste on biodegradability and mechanical properties bioplastic. In IOP Conference Series: Earth and Environmental Science, 679, 012013. https://doi.org/10.1088/1755-1315/679/1/012013

Ballesteros-Mártinez, L., Pérez-Cervera, C., & Andrade-Pizarro, R. (2020). Effect of glycerol and sorbitol concentrations on mechanical, optical, and barrier properties of sweet potato starch film. NFS journal, 20, 1-9. https://doi.org/10.1016/j.nfs.2020.06.002

Bashir, K., & Aggarwal, M. (2019). Physicochemical, structural and functional properties of native and irradiated starch: a review. Journal of food science and technology, 56, 513-523. https://doi.org/10.1007/s13197-018-3530-2

Cazón, P., Vázquez, M., & Velázquez, G. (2020). Regenerated cellulose films with chitosan and polyvinyl alcohol: Effect of the moisture content on the barrier, mechanical and optical properties. Carbohydrate polymers, 236, 116031. https://doi.org/10.1016/j.carbpol.2020.116031

Chen, D., Zhao, M., Tan, W., Li, Y., Li, X., Li, Y., & Fan, X. (2019). Effects of intramolecular hydrogen bonds on lipophilicity. European Journal of Pharmaceutical Sciences, 130, 100-106. https://doi.org/10.1016/j.ejps.2019.01.020

Department of Agriculture. (2021). Investment Guide for Cassava. Agribusiness and Marketing Assistance Service - Agribusiness Promotion Division. https://www.da.gov.ph/wp-content/uploads/2021/04/Investment-Guide-for-Cassava.pdf

Domene-López, D., García-Quesada, J. C., Martin-Gullon, I., & Montalbán, M. G. (2019). Influence of starch composition and molecular weight on physicochemical properties of biodegradable films. Polymers, 11(7), 1084. http://dx.doi.org/10.3390/polym11071084

Elhaes, H., Ezzat, H. A., Ibrahim, A., Samir, M., Refaat, A., & Ibrahim, M. A. (2024). Spectroscopic, Hartree–Fock and DFT study of the molecular structure and electronic

properties of functionalized chitosan and chitosan-graphene oxide for electronic applications. Optical and Quantum Electronics, 56(3), 458. https://doi.org/10.1007/s11082-023-05978-0

Fatima, S., Khan, M. R., Ahmad, I., & Sadiq, M. B. (2024). Recent advances in modified starch based biodegradable food packaging: A review. Heliyon, 10(6), e27453. https://doi.org/10.1016/j.heliyon.2024.e27453

Feky, A. R. E., Ismaiel, M., Yılmaz, M., Madkour, F. M., Nemr, A. E., & Ibrahim, H. a. H. (2024). Biodegradable plastic formulated from chitosan of Aristeus antennatus shells with castor oil as a plasticizer agent and starch as a filling substrate. Scientific Reports, 14(1), 11161. https://doi.org/10.1038/s41598-024-61377-9

Flores, J. M., Gallardo, A. K. R., Barba, B. J. D., & Tranquilan-Aranilla, C. (2024). Effect of ionizing radiation on the physicochemical and functional properties of silicone rubber and silicone foley catheter. Radiation Physics and Chemistry, 216, 111356. https://dx.doi.org/10.2139/ssrn.4540861

Fronza, P., Costa, A. L. R., Franca, A. S., & de Oliveira, L. S. (2023). Extraction and characterization of starch from cassava peels. Starch-Stärke, 75(3-4), 2100245. http://dx.doi.org/10.1002/star.202100245

Garces, V., García-Quintero, A., Lerma, T. A., Palencia, M., Combatt, E. M., & Arrieta, Á. A. (2021). Characterization of cassava starch and its structural changes resulting of thermal stress by functionally-enhanced derivative spectroscopy (FEDS). Polysaccharides, 2(4), 866-877. https://doi.org/10.3390/polysaccharides2040052

Gerassimidou, S., Martin, O. V., Diaz, G. Y. F., Wan, C., Komilis, D., & Iacovidou, E. (2022). Systematic Evidence Mapping to Assess the Sustainability of Bioplastics Derived from Food Waste: Do We Know Enough? Sustainability, 15(1), 611. https://doi.org/10.3390/su15010611

Gharbi, F. Z., Bougdah, N., Belhocine, Y., Sbei, N., Rahali, S., Damous, M., & Seydou, M. (2023). Green and Fast Extraction of Chitin from Waste Shrimp Shells: Characterization and Application in the Removal of Congo Red Dye. Separations, 10(12), 599. https://doi.org/10.3390/separations10120599

González-Torres, B., Robles-García, M. Á., Gutiérrez-Lomelí, M., Padilla-Frausto, J. J., Navarro-Villarruel, C. L., Del-Toro-Sánchez, C. L., ... & Reynoso-Marín, F. J. (2021). Combination of sorbitol and glycerol, as plasticizers, and oxidized starch improves the physicochemical characteristics of films for food preservation. Polymers, 13(19), 3356. https://doi.org/10.3390/polym13193356

Guzman-Puyol, S., Tedeschi, G., Goldoni, L., Benítez, J. J., Ceseracciu, L., Koschella, A., Heinze, T., Athanassiou, A., & Heredia-Guerrero, J. A. (2022). Greaseproof, hydrophobic, and biodegradable food packaging bioplastics from C6-fluorinated cellulose esters. Food Hydrocolloids, 128, 107562. https://doi.org/10.1016/j.foodhyd.2022.107562

Jaderi, Z., Tabatabaee Yazdi, F., Mortazavi, S. A., & Koocheki, A. (2023). Effects of glycerol and sorbitol on a novel biodegradable edible film based on Malva sylvestris flower gum. Food Science & Nutrition, 11(2), 991-1000. https://doi.org/10.1002/fsn3.3134

Jõgi, K., & Bhat, R. (2020). Valorization of food processing wastes and by-products for bioplastic production. Sustainable Chemistry and Pharmacy, 18, 100326. https://doi.org/10.1016/j.scp.2020.100326

Kowser, Md. A., Mahmud, H., Chowdhury, M. A., Hossain, N., Mim, J. J., & Islam, S. (2025). Fabrication and characterization of corn starch based bioplastic for packaging applications. Results in Materials, 25, 100662. https://doi.org/10.1016/j.rinma.2025.100662

Kusumaningrum, M., Imani, N. A. C., Gemilang, S., Rahma, F. N., & Wulansarie, R. (2023, June). Synthesis and Physical Characterization of Bioplastics Based on Jicama Starch (Pachyrhizur Erosus)–Chitosan.: Earth and Environmental Science, 1203(1), 012001. https://doi.org/10.1088/1755-1315/1203/1/012001

Lerbret, A., Mason, P. E., Venable, R. M., Cesàro, A. T. T. I. L. I. O., Saboungi, M. L., Pastor, R. W., & Brady, J. W. (2009). Molecular dynamics studies of the conformation of sorbitol. Carbohydrate research, 344(16), 2229-2235. http://dx.doi.org/10.1016/j.carres.2009.08.003

Li, B., Elango, J., & Wu, W. (2020). Recent advancement of molecular structure and biomaterial function of chitosan from marine organisms for pharmaceutical and nutraceutical application. Applied Sciences, 10(14), 4719. https://doi.org/10.3390/app10144719

Lomelí-Ramírez, M. G., Kestur, S. G., Manríquez-González, R., Iwakiri, S., de Muniz, G. B., & Flores-Sahagun, T. S. (2014). Bio-composites of cassava starch-green coconut fiber: Part II—Structure and properties. Carbohydrate Polymers, 102, 576–583. https://doi.org/10.1016/j.carbpol.2013.11.020

Miles, K. B., Ball, R. L., & Matthew, H. W. T. (2016). Chitosan films with improved tensile strength and toughness from N-acetyl-cysteine mediated disulfide bonds. Carbohydrate polymers, 139, 1-9. https://doi.org/10.1016/j.carbpol.2015.11.052

Mofokeng, J. P., Luyt, A. S., Tábi, T., & Kovács, J. (2012). Comparison of injection moulded, natural fibre-reinforced composites with PP and PLA as matrices. Journal of Thermoplastic Composite Materials, 25(8), 927-948. http://dx.doi.org/10.1177/0892705711423291

Mohammed, A. A., Hasan, Z., Borhana Omran, A. A., M Elfaghi, A., Khattak, M. A., Ilyas, R. A., & Sapuan, S. M. (2023). Effect of Various Plasticizers in Different Concentrations on: Physical, Thermal, Mechanical, and Structural Properties of: Wheat Starch-Based Films. Polymers, 15(1), 63. https://doi.org/10.3390/polym15010063

Mohan, K., Ganesan, A. R., Ezhilarasi, P. N., Kondamareddy, K. K., Rajan, D. K., Sathishkumar, P., Rajarajeswaran, J. & Conterno, L. (2022). Green and eco-friendly approaches for the extraction of chitin and chitosan: A review. Carbohydrate Polymers, 287, 119349. https://doi.org/10.1016/j.carbpol.2022.119349

Mutmainna, I., Tahir, D., Gareso, P. L., & Ilyas, S. (2019). Synthesis composite starch-chitosan as biodegradable plastic for food packaging. Physics, 1317, 012053. https://doi.org/10.1088/1742-6596/1317/1/012053

National Institute of Science and Technology. (2022). D-Optimal designs. Engineering Statistics Handbook. 5.5.2.1. https://doi.org/10.18434/M32189

Ncube, L. K., Ude, A. U., Ogunmuyiwa, E. N., Zulkifli, R., & Beas, I. N. (2020). Environmental Impact of Food Packaging Materials: A Review of Contemporary Development from Conventional Plastics to Polylactic Acid Based Materials. Materials (Basel), 13(21), 4994. https://doi.org/10.3390/ma13214994

Nigam, S., Das, A. K., & Patidar, M. K. (2021). Synthesis, characterization and biodegradation of bioplastic films produced from Parthenium hysterophorus by incorporating a plasticizer (PEG600). Environmental Challenges, 5, 100280. https://doi.org/10.1016/j.envc.2021.100280

Nirmal, N. P., Santivarangkna, C., Rajput, M. S., & Bengakul, S. (2020). Trends in shrimp processing waste utilization: An industrial prospective. Trends in Food Science & Technology, 103, 20-35. https://doi.org/10.1016/j.tifs.2020.07.001

Oghenejoboh, K. M., Orugba, H. O., Oghenejoboh, U. M., & Agarry, S. E. (2021). Value added cassava waste management

and environmental sustainability in Nigeria: A review. Environmental Challenges, 4, 100127. https://doi.org/10.1016/j.envc.2021.100127

Oluwasina, O. O., Akinyele, B. P., Olusegun, S. J., Oluwasina, O. O., & Mohallem, N. D. (2021). Evaluation of the effects of additives on the properties of starch-based bioplastic film. SN Applied Sciences, 3, 1-12. https://doi.org/10.1007/s42452-021-04433-7

Oluwasina, O., Aderibigbe, A., Ikupoluyi, S., Oluwasina, O., & Ewetumo, T. (2024). Physico-electrical properties of starch-based bioplastic enhanced with acid-treated cellulose and graphene oxide fillers. Sustainable Chemistry for the Environment, 6, 100093. https://doi.org/10.1016/j.scenv.2024.100093

Ooi, Z. X., Ismail, H., Bakar, A. A., & Aziz, N. A. A. (2012). The Comparison Effect of Sorbitol and Glycerol as Plasticizing Agents on the Properties of Biodegradable Polyvinyl Alcohol/Rambutan Skin Waste Flour Blends. Polymer-Plastics Technology and Engineering, 51(4), 432–437. https://doi.org/10.1080/03602559.2011.639827

Pakizeh, M., Moradi, A., & Ghassemi, T. (2021). Chemical extraction and modification of chitin and chitosan from shrimp shells. European Polymer Journal, 159, 110709. https://doi.org/10.1016/j.eurpolymj.2021.110709

Pelissari, F. M., Yamashita, F., Garcia, M. A., Martino, M. N., Zaritsky, N. E., & Grossmann, M. V. E. (2012). Constrained mixture design applied to the development of cassava starch–chitosan blown films. Journal of Food Engineering, 108(2), 262-267. https://doi.org/10.1016/j.jfoodeng.2011.09.004

Pither, R.J. (2003). CANNING | Quality Changes During Canning. In Caballero B. (Ed.) Encyclopedia of Food Sciences and Nutrition, 2, 845-85. https://doi.org/10.1016/B0-12-227055-X/00163-2

Preethi, R., R, A. N., Murthy, P. S. K., & Reddy, J. P. (2024). Utilization of tamarind kernel powder for the development of bioplastic films: production and characterization. Sustainable Food Technology. https://doi.org/10.1039/d4fb00199k

Pujiono, P., & Nurhayati, A. (2020). Effects of Glycerol and Chitosan Doses for Cassava Peels Organic Waste as Bioplastic Food Packaging and The Effects on Physical and Microbiological Food Quality. Sapporo Medical Journal, 54(9), 1-11. https://www.maejournal.com/volume/SMJ/54/09/effects-of-glycerol-and-chitosan-doses-for-cassava-peels-organic-waste-as-bioplastic-food-packaging-and-the-effects-on-physical-and-microbiological-food-quality-5fa2cd514e4df.pdf

Rajesh, A. (2023, October 23). Ecofriendly Polymeric Material: Paving The Way For Circular Bio-Economy; The Effect of Chitosan on Biodegradability and Water Resistance of Starch based Bioplastic. Society for Science. https://www.societyforscience.org/jic/2023-student-finalists/aswath-rajesh/

Ramadhan, M. O., & Handayani, M. N. (2020). The potential of food waste as bioplastic material to promote environmental sustainability: A review. Materials Science and Engineering, 980, 012082. https://dx.doi.org/10.1088/1757-899X/980/1/012082

Ritchie, H., Samborska, V., & Roser, M. (2023). Plastic Pollution. https://ourworldindata.org/plastic-pollution?insight=around-05-of-plastic-waste-ends-up-in-the-ocean#article-licence

Sangian, H. F., Maneking, E., Tongkukut, S. H. J., Mosey, H. I. R., Suoth, V., Kolibu, H., Tanauma, A., Pasau, G., As'ari, A., Masinambow, V. a. J., Sadjab, B. A., Sangi, M. M., & Rondonuwu, S. B. (2021). Study of SEM, XRD, TGA, and DSC of Cassava Bioplastics catalyzed by ethanol. Materials Science and Engineering, 1115(1), 012052. https://doi.org/10.1088/1757-899x/1115/1/012052

Selvam, A., Ilamathi, P. M. K., Udayakumar, M., Murugesan, K., Banu, R. J., Khanna, Y., & Wong, J. (2021). Food Waste Properties. Current Developments in Biotechnology

and Bioengineering, 11-41. http://dx.doi.org/10.1016/B978-0-12-819148-4.00002-6

Shafqat, A., Al-Zaqri, N., Tahir, A., & Alsalme, A. (2021). Synthesis and characterization of starch based bioplatics using varying plant-based ingredients, plasticizers and natural fillers. Saudi Journal of Biological Sciences, 28(3), 1739-1749. https://doi.org/10.1016/j.sjbs.2020.12.015

Shen, X. L., Wu, J. M., Chen, Y., & Zhao, G. (2010). Antimicrobial and physical properties of sweet potato starch films incorporated with potassium sorbate or chitosan. Food Hydrocolloids, 24(4), 285-290. https://doi.org/10.1016/j.jfoodeng.2011.09.004

Tan, S. X. ,Ong H. C. , Andriyana A., Lim S., Pang Y. L., Kusumo F., & Ngoh G. C. (2022). Characterization and Parametric Study on Mechanical Properties Enhancement in Biodegradable Chitosan-Reinforced Starch-Based Bioplastic Film. Polymers, 14(2), 278-294. https://doi.org/10.3390/polym14020278

TA Instruments. (2025). TA Instruments Materials Science - TA Instruments. TA Instruments - Materials Science Solutions. https://www.tainstruments.com/

Thuppahige, V. T. W., Moghaddam, L., Welsh, Z. G., Wang, T., Xiao, H. W., & Karim, A. (2023). Extraction and characterisation of starch from cassava (Manihot esculenta) agro-industrial wastes. LWT, 182, 114787. https://doi.org/10.1016/j.lwt.2023.114787

Tsang, Y. F., Kumar, V., Samadar, P., Yang, Y., Lee, J., Ok, Y. S., Song, H., Kim, K.-H., Kwon, E. E., & Jeon, Y. J. (2019). Production of bioplastic through food waste valorization. Environmental International, 127, 625-644. https://doi.org/10.1016/j.envint.2019.03.076

United Nations Environment Programme (UNEP). (2024, February 28). Global Waste Management Outlook 2024. https://sustainable.kmutt.ac.th/current-waste-problems-an-unfolding-global-crisis/

Vallejo-Domínguez, D., Rubio-Rosas, E., Aguila-Almanza, E., Hernández-Cocoletzi, H., Ramos-Cassellis, M. E., Luna-Guevara, M. L., ... & Show, P. L. (2021). Ultrasound in the deproteinization process for chitin and chitosan production. Ultrasonics Sonochemistry, 72, 105417. https://doi.org/10.1016/j.ultsonch.2020.105417

Varun, T. K., Senani, S., Jayapal, N., Chikkerur, J., Roy, S., Tekulapally, V. B., ... & Kumar, N. (2017). Extraction of chitosan and its oligomers from shrimp shell waste, their characterization and antimicrobial effect. Veterinary world, 10(2), 170. https://doi.org/10.14202/vetworld.2017.170-175

Wang, W., Wang, H., Jin, X., Wang, H., Lin, T., & Zhu, Z. (2018). Effects of hydrogen bonding on starch granule dissolution, spinnability of starch solution, and properties of electrospun starch fibers. Polymer, 153, 643-652. https://doi.org/10.1016/j.polymer.2018.08.067

Wang, X. Y., Wang, J., Zhao, C., Ma, L., Rousseau, D., & Tang, C. H. (2023). Facile fabrication of chitosan colloidal films with pH-tunable surface hydrophobicity and mechanical properties. Food Hydrocolloids, 137, 108429. https://doi.org/10.1016/j.foodhyd.2022.108429

Wang, X., Huang, L., Zhang, C., Deng, Y., Xie, P., Liu, L., & Cheng, J. (2020). Research advances in chemical modifications of starch for hydrophobicity and its applications: A review. Carbohydrate Polymers, 116292. https://doi.org/10.1016/j.carbpol.2020.116292

Wani, A. K., Akhtar, N., Mir, T. U. G., Rahayu, F., Suhara, C., Anjli, A., ... & Américo-Pinheiro, J. H. P. (2024). Eco-friendly and safe alternatives for the valorization of shrimp farming waste. Environmental Science and Pollution Research, 31(27), 38960-38989. https://doi.org/10.1007/s11356-023-27819-z

Widiarto, S., Yuwono, S. D., Rochliadi, A., & Arcana, I. M. (2017, February). Preparation and characterization of cellulose and nanocellulose from agro-industrial waste-cassava peel. Materials Science and Engineering 176(1), 012052. https://doi.org/10.1088/1757-899X/176/1/012052

William, W., & Wid, N. (2019). Comparison of extraction sequence on yield and physicochemical characteristic of chitosan from shrimp shell waste. Journal of Physics: Conference Series, 1358 012002. https://doi.org/10.1088/1742-6596/1358/1/012002

WRAP. (n.d.). Plastic Packaging. https://www.wrap.ngo/taking-action/plastic-packaging

Yan, Q., Hou, H., Guo, P., & Dong, H. (2012). Effects of extrusion and glycerol content on properties of oxidized and acetylated corn starch-based films. Carbohydrate Polymers, 87(1), 707–712. https://doi.org/10.1016/j.carbpol.2011.08.048

Zahiruddin, S.M.M., Othman, S.H., Tawakkal, I.S.M.A. & Talib, R.A. (2019). Mechanical and thermal properties of tapioca starch films plasticized with glycerol and sorbitol. Food Research 3(2), 157-163. https://doi.org/10.26656/fr.2017.3(2).105

Zhang, Y., Xie, J., Ellis, W. O., Li, J., Appaw, W. O., & Simpson, B. K. (2024). Bioplastic films from cassava peels: Enzymatic transformation and film properties. Industrial Crops and Products, 213, 118427. https://doi.org/10.1016/j.indcrop.2024.118427